Available online at www.sciencedirect.com
ScienceDirect
Trans. Nonferrous Met. Soc. China 25(2015) 2429−2437
Transactions of Nonferrous Metals Society of China
www.tnmsc.cn

Oxide film on bubble surface of aluminum foams produced by gas injection foaming process

Yu-tong ZHOU[1], Yan-xiang LI[1,2]

1. School of Materials Science and Engineering, Tsinghua University, Beijing 100084, China;
2. Key Laboratory for Advanced Materials Processing Technology, Ministry of Education, Tsinghua University, Beijing 100084, China

Received 23 September 2014; accepted 23 January 2015

Abstract: Based on A356 aluminum alloy, aluminum foams were prepared by gas injection foaming process with pure nitrogen, air and some gas mixtures. The oxygen volume fraction of these gas mixtures varied from 0.2% to 8.0%. Optical microscopy, scanning electron microscopy (SEM) and Auger electron spectroscopy (AES) were used to analyze the influence of oxygen content on cell structure, relative density, macro and micro morphology of cell walls, coverage area fraction of oxide film, thickness of oxide film and other aspects. Results indicate that the coverage area fraction of oxide film on bubble surface increases with the increase of oxygen content when the oxygen volume is less than 1.2%. While when the oxygen volume fraction is larger than 1.6%, an oxide film covers the entire bubble surface and aluminum foams with good cell structure can be produced. The thicknesses of oxide films of aluminum foams produced by gas mixtures containing 1.6%−21% oxygen are almost the same. The reasons why the thickness of oxide film nearly does not change with the variation of oxygen content and the amount of oxygen needed to achieve 100% coverage of oxide film are both discussed. In addition, the role of oxide film on bubble surface in foam stability is also analyzed.
Key words: aluminum foam; gas injection foaming process; oxide film; foam stability mechanism

1 Introduction

Gas injection foaming process was developed firstly by the Aluminum Company of Canada (Alcan) [1] and the Norwegian Norsk Hydro Company [2] at the end of 1980s. Aluminum foams produced by gas injection foaming process can be processed into sandwich composite, which is a kind of ideal energy absorption material [3]. The aluminum foam plates also can be used in sound absorption and noise reduction field [4]. So, aluminum foams produced by gas injection foaming process became a hot research topic in 1990s. During the past two decades, great progresses were achieved in the studies of foaming requirements [5,6], foaming parameters [7], mechanical property of aluminum foams [8] and other aspects. But aluminum foams produced by gas injection foaming process still suffer from non-uniformity of cell size and poor repeatability of manufacturing process, which exert negative influence on their large-scale commercial production. Such an embarrassing situation is a result of the reality that most of the findings come from empirical experiences, which makes us fail to gain a profound scientific knowledge of foam stability. In fact, researches on foam stability have been going on for many years, so the understanding of foam stability is also in gradual progress. In the 1990s, almost all researches focus on the particles. JIN et al [1] proposed the famous particles size and volume fraction window for producing foam and suggested that about 10% (volume fraction) 10 μm particles should be added into the melt to achieve the best foaming effect. LEITLMEIER et al [6] studied the relationship between the travelling distance of bubbles and foam stability. They found that a minimum travelling distance was needed to ensure the stability of foams when the particle volume fraction of melt is fixed. Entering the 21st century, the experiments conducted by BABSCÁN et al [9] reflected the importance of oxide film in foam stability. Therefore, at present, most researchers have a unanimous consensus that at least two requirements are needed to ensure the stability of foams: the segregation of particles on the bubble surface and the formation of oxide film on the bubble surface [10].

Foundation item: Project (51371104) supported by the National Natural Science Foundation of China
Corresponding author: Yan-xiang LI; Tel: +86-10-62773640; E-mail: yanxiang@tsinghua.edu.cn
DOI: 10.1016/S1003-6326(15)63859-6

In recent years, both from experiments and simulations, the effects of particles on foam stability were investigated deeply by a lot of researchers and some models were proposed [11−14]. As shown in Fig. 1, HAIBEI et al [15] summarized and classified these models and then presented their idea that particles improved foam stability by creating surface elasticity and increasing the apparent viscosity (Fig. 1(f)). On the contrary, only a few researches related to the role of oxide film in foam stability. BABSCÁN et al [16] produced aluminum foams with nitrogen, air and oxygen respectively. They found there was a layer of oxide film on the surface of bubble produced by the latter two gases and their stability was much better. The thickness of oxide film on bubble surface [16] and the oxidation behavior of oxide film [9] were studied as well. However, further information about the morphology of oxide film, the coverage area fraction of oxide film on bubble surface, the critical oxygen volume fraction needed to produce aluminum foams with good cell structure and the role of oxide film in foam stability have not been reported. In order to improve the gas injection foaming technology, those issues are studied through preparing aluminum foams by gas mixtures containing different oxygen contents.

2 Experimental

A356 aluminum alloy was used as raw materials. 10% Al_2O_3 particles, with an average size of 10 μm, were mixed into A356 alloy melt as foam stabilizer and were fully dispersed by mechanical stirring. In order to remove the engulfed air induced by stirring from the composite melt, the melt was refined and degassed by pure nitrogen. During the whole preparation process, foaming temperature was kept at 680−690 °C, the gas flow was 0.9−1.0 L/min. The orifice diameter of nozzle was about 0.5 mm. Compressed air and nitrogen were selected as foaming medium. The purity of nitrogen was over 99.99% (volume fraction). Gas flows of air and nitrogen were controlled by mass flowmeters independently. Thus, compressed air and nitrogen could be mixed at a given volume proportions by adjusting the gas flows of gas and nitrogen, ensuring the oxygen volume fraction of gas mixtures meet the requirements of tests. The selected nominal flows were injected into the melt to make aluminum foams. In order to control the oxidation time, aluminum foams were removed from the surface of the melt in 50 s. In our experiments, aluminum foams were produced by pure nitrogen, air and gas mixtures at the platform built by ourselves [17]. Since the foam stability under some experimental conditions was poor, an auxiliary measure of lifting the aluminum foams was adopted during the sample collection process. Nitrogen, air and gas mixtures containing 0.2%−8.0% oxygen were used to represent those experimental gases hereinafter.

According to ISO standard 2896−86, the average cell size was obtained by line method. Chord lengths of three-dimensional directions were firstly measured by a ruler, and then the average cell size could be calculated by

$$D=L/0.616 \tag{1}$$

where D is the average cell size and L is the average chord length. The relative densities of aluminum foams were measured as well. The data could be obtained by

$$\rho_r=m_f/(V_f\,\rho_s) \tag{2}$$

where ρ_r is the relative density, m_f is the mass of aluminum foam, V_f is the volume of aluminum foam and ρ_s is the density of A356 aluminum alloy.

In order to observe the original macro and micro morphology of cell walls, several cell wall specimens were randomly cut from aluminum foams and their images were obtained by Axio scope a1 optical microscopy and Quanta 200 scanning electron microscopy. The elements content depth profile analyses

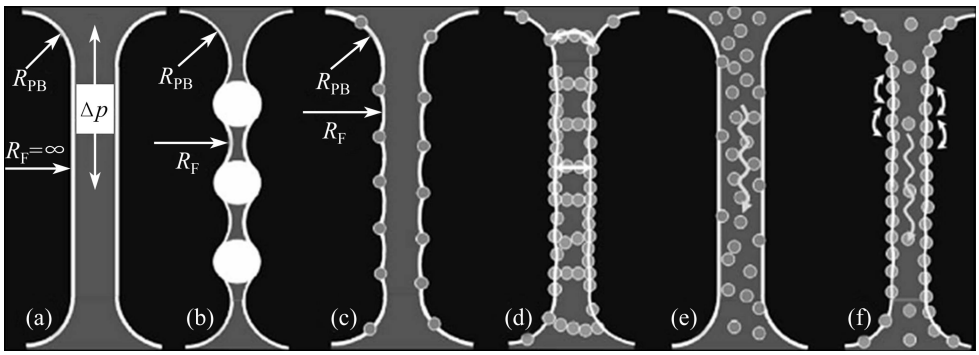

Fig. 1 Summary of effects of particles on different models for foam stability [15]: (a) Liquid film in foam; (b) Adsorbed particles bridged by film; (c) Interfaces modulated by adsorbed particles; (d) Particle layers at interfaces mechanically connected by bridges; (e) Drainage reduction by particles; (f) Creating surface elasticity and increasing viscosity

of oxide films were carried out by PHI−700 Auger electron spectroscopy to determine the thicknesses of oxide films. The analyses only focus on the atomic contents of Al and O (regarding the total number of atoms of these two elements as 100%). Two or three cell walls of aluminum foams produced under each experimental condition were selected as analysis objects. A characteristic region was selected in these areas covered with an oxide film. The dimensions of characteristic region were 10 μm × 10 μm.

3 Results

3.1 Influence of oxygen content on cell structure and relative density

Aluminum foams produced by gas mixtures containing different oxygen contents were cut by an electric discharge cutting machine. Their vertical sections are shown in Fig. 2. We can see from this graph that with the increase of oxygen content, cell structure of aluminum foam becomes more uniform and the number of large cells (whose size is 2 times larger the average size) decreases significantly, indicating that the foam stability is improved. When the oxygen volume fraction is 1.6%, large cells in the structure disappear completely. Aluminum foams prepared under that condition seem identical to the samples blown by air, which suggests that aluminum foams with good cell structure can be produced when the oxygen volume fraction is larger than 1.6%. In order to reflect the effect of oxygen content on foam stability directly, air and nitrogen were used sequentially in preparation of the same aluminum foam. At first, only air was blown into the melt. After that, we turned off air and blew nitrogen to produce aluminum foam. The vertical section of that sample is shown in Fig. 3. Obviously, the cell structure of upper part is good, and cell size is uniform. While intact cell cannot be found in the lower part due to the rupture, collapse and coalescence of cells. Such a sharp contrast certifies that the formation of oxide film on bubble surface constitutes an indispensable part of foam stability in gas injection foaming process.

In Fig. 4, the statistics show that with the increase of oxygen volume fraction, the average cell size reduces gradually and the relative density rises slightly. Furthermore, both of the parameters tend to be stable when the oxygen volume fraction is greater than 1.6%.

3.2 Influence of oxygen content on macro and micro morphology of cell walls

The macro morphology of cell walls of aluminum foams produced by gas mixtures containing different oxygen contents was studied carefully. Their typical appearances are shown in Fig. 5. It can be seen from the figures that the colors of cell walls of aluminum foams produced by gas mixtures containing different oxygen

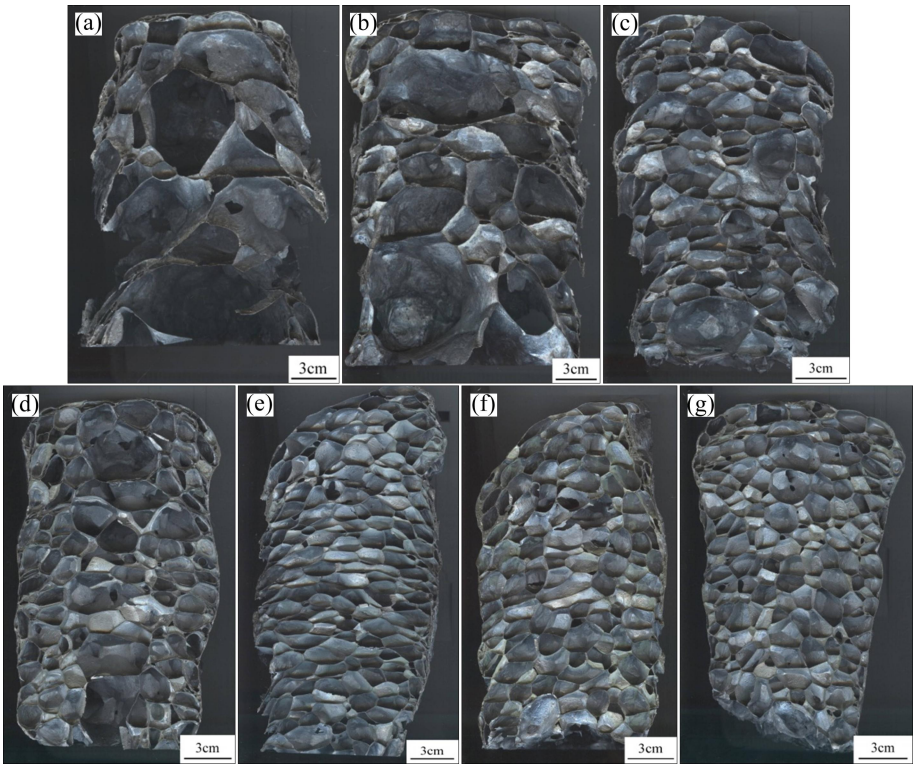

Fig. 2 Vertical sections of aluminum foams produced by gas mixtures containing different oxygen contents: (a) Pure nitrogen; (b) 0.4% oxygen; (c) 0.8% oxygen; (d) 1.2% oxygen; (e) 1.6% oxygen; (f) 2.0% oxygen; (g) Air

Fig. 3 Vertical section of aluminum foam produced by air and nitrogen sequentially

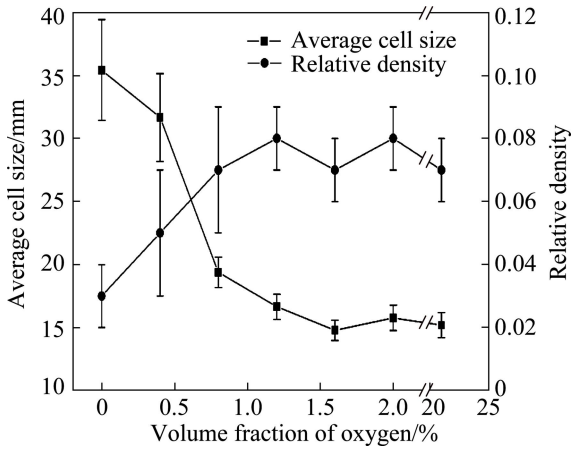

Fig. 4 Average cell size and relative density as function of oxygen volume fraction

contents are obviously distinct. Specifically, when the oxygen volume fraction of gas mixtures is less than 0.2%, almost all the bubble surface is dark grey. Some silvery regions start to appear on bubble surfaces and coexist with dark grey regions when the oxygen volume fraction increases to 0.4%−1.0%. Furthermore, with the increase of oxygen volume fraction, the area of dark grey regions decreases, while that of silvery regions increases rapidly. When the oxygen volume fraction of gas mixtures is larger than 1.2%, dark grey regions disappear and the whole bubble surface is silvery. After that, the color of cell walls no longer changes significantly.

The micro morphology of cell walls of aluminum foams produced by gas mixtures containing different oxygen contents was studied with SEM (Fig. 6). When nitrogen or gas mixture containing 0.2% oxygen is used, the oxidized area on bubble surface is very small. Bare Al_2O_3 particles are distributed uniformly and densely on the bubble surface (Figs. 6(a) and (b)). These particles combine with the bubble surface very well and they cannot be easily detached from the surface by external force. When the oxygen volume fraction of gas mixtures increases to 0.4%−1.0%, the coverage area of oxide film increases gradually (Figs. 6(c) and (d)). So, we can find regions covered with an oxide film and exposed regions coexisting in the same field. In contrast to particles densely accumulating on the exposed region, almost no particle attaches to the surface of oxide film. An undulating oxide film covers the entire bubble surface and many white river patterns are formed when the oxygen volume fraction increases to 1.2%. These exposed regions covered with many Al_2O_3 particles disappear at the same time (Fig. 6(e)). Almost all these river patterns disappear when air is used to produce the aluminum foams and the film becomes smoother (Fig. 6(f)).

3.3 Influence of oxygen content on thickness of oxide films

AES depth profiles penetrating cell walls are shown in Fig. 7. Since the elemental composition of oxide film

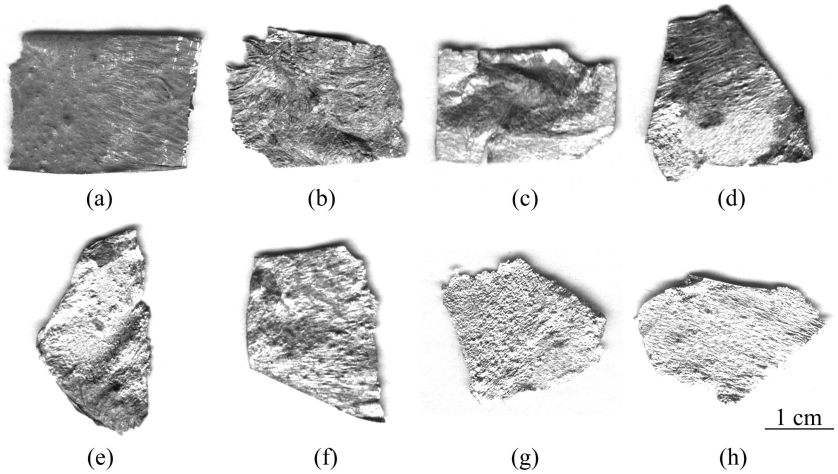

Fig. 5 Macro morphology of cell walls of aluminum foams produced by gas mixtures containing different oxygen contents: (a) Pure nitrogen; (b) 0.2% oxygen; (c) 0.4% oxygen; (d) 0.6% oxygen; (e) 0.8% oxygen; (f) 1.0% oxygen; (g) 1.2% oxygen; (h) Air

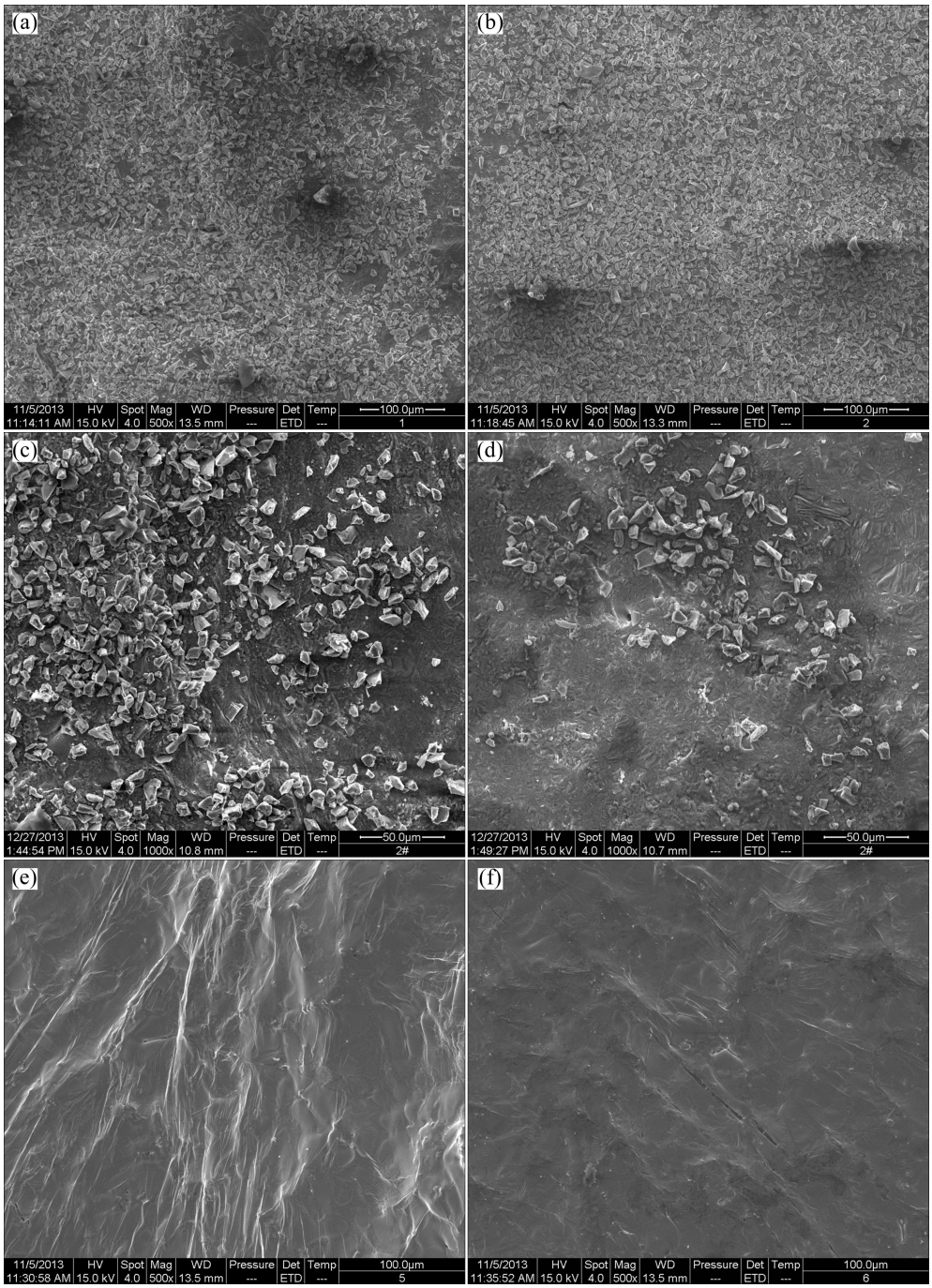

Fig. 6 Micro morphology of cell walls of aluminum foams produced by gas mixtures containing different oxygen contents: (a) Pure nitrogen; (b) 0.2% oxygen; (c) 0.6% oxygen; (d) 0.8% oxygen; (e) 1.2% oxygen; (f) Air

is severely affected by the particles densely distribute on bubble surface, so the aluminum foams produced by gas mixtures containing more than 1.6% oxygen are studied. As can be seen from these graphs, the tendencies of two elements are distinct. More precisely, the content of O drops significantly with etching, while that of Al increases gradually at the same time. During the etching process, large fluctuation cannot be found in the two curves, which proves that the composition of oxide film does not suffer mutation. Although the oxygen volume fraction varies from 1.6% to 21%, all the results show that the content of O starts to decline and that of Al begins to rise at a similar depth. In this sense, oxide films on bubble surface are penetrated at that depth, and then the elemental content gradually transits to the composition of A356 aluminum alloy. Since the etching rate is constant, it takes similar time to penetrate oxide films on bubble surface, suggesting that the thicknesses of all the oxide films are roughly equal. In other words, the thickness of oxide film does not increase with the increase of oxygen volume fraction. Because the contents of O in Al_2O_3, MgO and $MgAl_2O_4$ (the main

compositions of the oxide film of A356 aluminum alloy) are all located in the range of 50%−60%, we regard the time that when the mole fraction of O decreases to below 60% as the symbol of penetration of oxide film on bubble surface. As can be seen from Fig. 7, the thicknesses of oxide films of aluminum foams produced by gas mixtures containing 1.6%−21% oxygen are about 14.0−15.5 nm, the mean value of which is 14.7 nm.

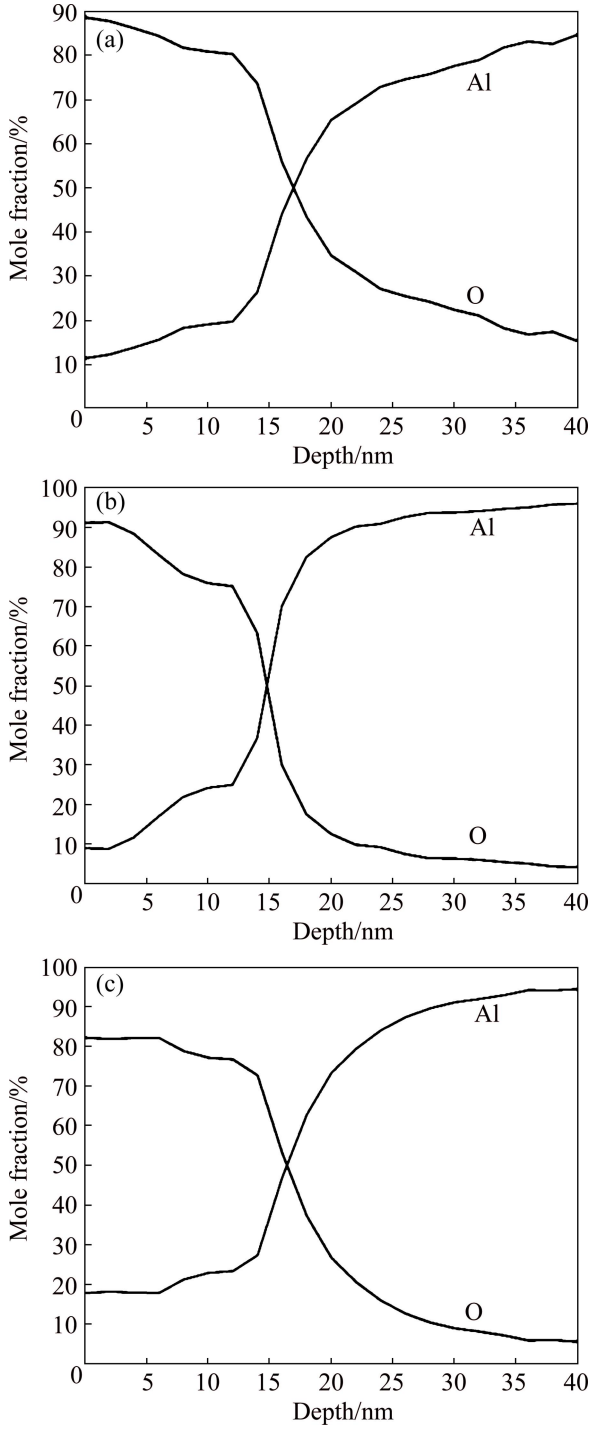

Fig. 7 AES depth profile penetrating cell walls of aluminum foams produced by gas mixtures containing different oxygen contents: (a) 1.6% oxygen; (b) 8.0% oxygen; (c) Air

4 Discussion

4.1 Oxidation process of aluminum alloy

As a kind of common aluminum alloy, the oxidation kinetics of A356 aluminum alloy has been studied deeply. NEWKIRK et al [18] proposed a reaction channel model to explain how the oxide particles can be continuously formed. YANG et al [19] suggested that Mg could damage the dense Al_2O_3 film and keep the melt exposed to the air. While Si could take part in the circular reactions and accelerate the rate of oxidation reactions significantly. In addition, these two elements needed to work together. It would not work if there was a lack of any kind of element. However, compared with normal oxidation process, there are mainly two big differences existing in the gas injection forming. On one hand, the oxidation time is very short. The oxidation process only starts from the bubble forming at the nozzle and ends at bubble solidifying on the surface of the melt. On the other hand, the gas which can react with bubble surface is limited. It is acknowledged that aluminum foam is a kind of closed cell porous metal, so gas is enclosed in each independent cell. Accordingly, we believe that bubble surface cannot react with the gases in the atmospheric environment on the ground that oxidation process is relatively quick.

Oxidation kinetics suggests that the oxidation process of metals is often affected by several factors, such as temperature, oxygen pressure, time and especially the type of metal. The PBR value of Al is 1.28 [20], which means that the protection of Al_2O_3 film is very good. The oxidation rate of oxide film with good protection is controlled by the mass transfer process of metal atoms or oxygen atoms and follows a square root law (Eq. (3)) [21]:

$$x^2=k_p t \tag{3}$$

where x is the thickness of oxide film, k_p is parabolic velocity constant and t is oxidation time. WAGNER [21] found quantitative relationships between the parabolic velocity constant and partial pressure of oxygen. For Al_2O_3, which belongs to metal ion excess oxides (namely n-type conductivity), the mathematical relation between its parabolic velocity constant and oxygen partial pressure is shown as Eq. (4) [21]:

$$k_p = C\left[\left(\frac{1}{p'_{O_2}}\right)^{1/4} - \left(\frac{1}{p''_{O_2}}\right)^{1/4}\right] \tag{4}$$

where C is a constant, p'_{O_2} means the equilibrium oxygen partial pressure at metal/oxide film interface, p''_{O_2} means oxygen partial pressure of atmosphere. According to the knowledge of thermodynamics, the

equilibrium oxygen partial pressure p'_{O_2} of chemical reaction (5) can be calculated by Eqs. (6)−(11).

$$2Al(l)+(3/2)O_2(g) \rightleftharpoons Al_2O_3(s) \quad (5)$$

$$\Delta_r G_m^{\Theta} = \sum v_B G_B^{\Theta} \quad (6)$$

$$\mu_B^{\Theta} = G_B^{\Theta} = H_B^{\Theta} - TS_B^{\Theta} \quad (7)$$

$$\mu_B = \mu_B^{\ominus} + RT\ln(p_B/p^{\Theta}) \quad (8)$$

$$\mu_B = \mu_B^{\ominus} + RT\ln x_B \quad (9)$$

$$\Delta_r G_m^{\Theta} = -RT\ln K^{\Theta} \quad (10)$$

$$K^{\Theta} = \prod_B (p_B/p^{\Theta})^{v_B} \quad (11)$$

where l, g and s mean liquid, gas and solid, respectively; $\Delta_r G_m^{\Theta}$ is standard mole reaction Gibbs function; v_B is the stoichiometric coefficient of substance B in chemical reaction (5), G_B^{Θ} is standard mole Gibbs free energy of substance B; μ_B^{Θ} is standard chemical potential of substance *B*; H_B^{Θ} is standard mole enthalpy of substance *B*, S_B^{Θ} is standard mole entropy of substance B, *T* is temperature; μ_B is chemical potential of substance *B*; *R* is mole gas constant; p_B is partial pressure of gas B, p^{Θ} is standard atmospheric pressure; x_B is mole fraction of liquid B; K^{Θ} is standard equilibrium constant. All the data needed for calculation can be acquired by seeking handbook of thermodynamic data [22]. When the gas mixture containing 1.0% oxygen was blown into A356 aluminum alloy melt at 1000 K, the equilibrium oxygen partial pressure of chemical reaction (5) is about 4.62×10^{-41} Pa. Therefore, p''_{O_2} of this experiment is far greater than p'_{O_2}, so Eq. (4) can be simplified into Eq. (12):

$$k_p = C\left(\frac{1}{p'_{O_2}}\right)^{1/4} \quad (12)$$

Apparently, the parabolic velocity constant has nothing to do with oxygen partial pressure. In other words, oxygen content of gas mixture exerts no influence on k_p. Referring to Eq. (3), we come to a conclusion that the thickness of oxide film is only determined by oxidation time. Because experimental conditions are identical, the oxidation time of different preparation processes are almost the same. In summary, from the perspective of theoretical prediction, the thicknesses of oxide films of aluminum foams produced by gas mixtures containing different oxygen contents should be nearly equal. This is consistent with the experimental results.

4.2 Amount of oxygen needed for oxidation process

The oxidation reaction occurred on bubble surface will consume oxygen of gas mixtures, and the oxidation process cannot continue when oxygen is depleted. In the experiments, we can observe the experimental phenomenon that coverage area fraction of oxide film on bubble surface increases with the increase of oxygen volume fraction of gas mixtures. Thus, studying the amount of oxygen required for oxidation process theoretically is a good complement to the experimental studies. Foaming gases will be heated when they flow through the pipeline or rise in the melt. So, based on the research conducted by FAN et al [23], we consider that the temperature of gas is equal to that of the melt when bubbles rise to the surface of the melt (the ideal mole gas volume under the condition of 953 K is 78.2 L). In addition, the amount of oxygen required for oxidation process is related to the composition of the oxide film. Although Mg contained in A356 aluminum alloy would substantially affect the oxidation rate and the composition of oxide film, making the oxide film on bubble surface is mainly composed of MgO, $MgAl_2O_4$ and Al_2O_3 [24]. However, the densities and mass fractions of O in its oxidation products MgO and $MgAl_2O_4$ are similar with Al_2O_3. For the convenience of calculation, the density and the oxygen mass fraction in oxide film are regarded as 3.8 g/cm^3 and 0.43, respectively. If the shape of bubble is spherical, the amount of oxygen required to oxidize a 14.7 nm thick oxide film on the entire surface of a 16 mm diameter bubble can be calculated by

$$\varphi_{O_2} = 3h\rho_f\omega_O V_g/(r\cdot M_{O_2}) \quad (13)$$

where φ_{O_2} is the critical oxygen volume fraction of gas mixture, *h* is the thickness of oxide film, ρ_f is the density of oxide film, ω_O is the oxygen mass fraction of oxide film, V_g is mole ideal gas volume, *r* is the radius of bubble and M_{O_2} is relative molar mass of oxygen. The results indicate that the theoretically critical oxygen volume fraction of gas mixture is 2.2%. During the process of adding ceramic particles, the A356 aluminum alloy melt reacts with air and some oxides are already formed，which reduces the amount of oxygen required for oxidation process. So, the experimental phenomenon that aluminum foams with good cell structure can be produced when the oxygen volume fraction of gas mixture is larger than 1.6%, is roughly consistent with the theoretically prediction.

4.3 Role of oxide film in foam stability

Overall, the thickness of oxide film will be larger than 10 nm when the oxygen volume fraction is 1.6%−21% and the thickness of oxide film will not increase with the increase of oxygen volume fraction of gas mixtures. In this sense, the oxide film with a certain thickness is enough to ensure the stability of foams.

Furthermore, it can be seen from the experimental results that coverage area fraction of oxide film on bubble surface also plays a pivotal role in keeping foams from rupture and collapse. Foam stability increases significantly with the increase of coverage area fraction of oxide film. It meets the requirements of producing aluminum foams with good cell structure immediately when an oxide film covers the entire bubble surface. In view of these phenomena, having a certain thickness and covering the entire bubble surface maybe two compulsory prerequisites of oxide film to improve foam stability.

From the micro perspective, we figure that compact and continuous oxide film, which is formed on the bubble surface, can help the bubble to resist external forces during the process of rising and accumulation. Its existence ensures the foams not to rupture when they suffer some disturbances, for example, liquid flows. Actually, the idea that Al_2O_3 film possesses a certain extent of strength is confirmed by experiments already. Nanoindentation shows that the elastic modulus of Al_2O_3 nano flakes is about 250 GPa [25]. On the contrary, without the protection of oxide film, the exposed regions are apt to be the weak points of bubbles, which would lead to the rupture of foams. That is the reason why substantial increase of foam stability can be acquired when the coverage area fraction of oxide film reaches 100%.

5 Conclusions

1) Formation of oxide film on bubble surface constitutes an indispensable part of foam stability in gas injection foaming process. Aluminum foams with good cell structure can be produced when the oxygen volume fraction of gas mixture is larger than 1.6%.

2) With the increase of oxygen volume fraction, the coverage area fraction of oxide film increases and the color of cell walls changes from dark grey to silvery. An oxide film covers the entire bubble surface when the oxygen volume fraction of gas mixture is larger than 1.2%. Bare Al_2O_3 particles uniformly and densely distribute on the surface of these regions which is not covered with an oxide film, while few particle attaches to the surface of those regions covered with an oxide films.

3) When the oxygen volume fraction is 1.6%−21%, the thickness of oxide film nearly does not change with the increase of oxygen content. The thicknesses of oxide films vary from 14.0 to 15.5 nm and the mean value is 14.7 nm. The study of oxidation kinetics of Al_2O_3 film also suggests that the thickness of oxide film has nothing to do with the oxygen volume fraction of gas mixture.

4) Theoretical calculations show that the oxygen volume fraction of gas mixture which can meet the requirement of oxidation process is 2.2%. This value is roughly consistent with the experimental phenomenon.

5) Having a certain thickness and covering the entire bubble surface maybe two compulsory prerequisites of oxide film to improve foam stability. Compact and continuous oxide film, which possesses a certain extent of strength, can significantly improve the stability of foams by helping them to resist external forces and disturbances.

Acknowledgment

The authors would also like to thank Jian-yu YUAN for his technical assistance.

References

[1] JIN I, KENNY L D, SANG H. Method of producing lightweight foamed metal: USA Patent 4973358 [P]. 1990−11−27.

[2] RUCH W W, KIRKEVAG B. A process of manufacturing particle reinforced metal foam and product thereof: European, Patent 0483184 [P]. 1994−02−07.

[3] HAN M S, CHO J U. Impact damage behavior of sandwich composite with aluminum foam core [J]. Transactions of Nonferrous Metals Society of China, 2014, 24(S): s42−s46.

[4] FAN Xue-liu, CHEN Xiang, LIU Xing-nan, LI Yan-xiang. Properties of aluminum foam prepared by gas injection method [J]. The Chinese Journal of Nonferrous Metals, 2011, 21(6): 1320−1327. (in Chinese)

[5] IP S W, WANG Y, TOGURI J M. Aluminum foam stabilization by solid particles [J]. Canadian Metallurgical Quaeterly, 1999, 38: 81−92.

[6] LEITLMEIER D, DEGISCHER H P, FLANKL H J. Development of a foaming process for particulate reinforced aluminum melts [J]. Advance Engineering Materials, 2002, 4(10): 735−740.

[7] WANG De-qing, SHI Zi-yuan. Effect of ceramic particle on cell size and wall thickness of aluminum foam [J]. Materials Science & Engineering A, 2003, 361: 45−49.

[8] PRAKASH O, SANG H, EMBURY J D. Structure and properties of Al−SiC foam [J]. Materials Science & Engineering A, 1995, 199: 195−203.

[9] BABCSÁN N, LEUTLMEIER D, DEGISCHER H P, BANHART J. The role of oxidation in blowing particle-stabilized aluminum foams [J]. Advanced Engineering Materials, 2004, 6(6): 421−428.

[10] BANHART J. Light-metal foams−history of innovation and technological challenges [J]. Advanced Engineering Materials, 2013, 15(3): 82−111.

[11] KÖRNER C. Foam formation mechanisms in particles suspensions applied to metal foams [J]. Materials Science & Engineering A, 2008, 495: 227−235.

[12] KAPTAY G. Interfacial criteria for stabilization of liquid foams by solid particles [J]. Colloids and Surface A, 2004, 230: 67−80.

[13] GERGELY V, CLYNE T W. Drainage in standing liquid metal foams: Modeling and experimental observations [J]. Acta Materialia, 2004, 52: 3047−3058.

[14] KLINTER A J, LEON C A, DREW R A L. The optimum contact angle range for metal foam stabilization: An experimental comparison with the theory [J]. Journal of Materials Science, 2010, 45: 2174−2180.

[15] HAIBEL A, RACK A, BANHART J. Why are metal foams stable [J]. Applied Physical Letter, 2006, 89: 154102−154104.

[16] BABCSÁN N, LEITLMEIER D, DEGISCHER H P. Foamability of particle reinforced aluminum melt [J]. Materialwissenschaft Und Werkstofftechnik, 2003, 34: 22−29.

[17] LIU Xing-nan, LI Yan-xiang, CHEN Xiang. Foam stability in gas injection foaming process [J]. Journal Materials Science, 2010, 45: 6481−6493.
[18] NEWKIRK M S, URQUHART A W, ZWICHER H R. Formation of Lanxide ceramic composite materials [J]. Journal of Materials Research, 1986, 1(1): 81−89.
[19] YANG Liu, ZHU De-gui, XU Chang-qing, ZHANG Jun, ZHANG Jian. On the role of magnesium and silicon in formation of alumina from aluminum alloy by means of DIMOX processing [J]. Metallurgical and Materials Transaction A, 1996, 27: 2094−2099.
[20] PILLING N B, BEDWORTH R E. The oxidation of metals at high temperature [J]. Journal of the Institute of Metals, 1923, 29: 529−591.
[21] KOFSTAD P. High temperature corrosion [M]. London, UK: Elsevier Applied Science Publishers Ltd, 1988.
[22] LIANG Ying-jiao, CHE Meng-chang. Handbook of the thermodynamics data for inorganic substances [M]. Shenyang: Northwestern University Press, 1993. (in Chinese)
[23] FAN Xue-liu, CHEN Xiang, LIU Xing-nan, ZHANG Hui-ming, LI Yan-xiang. Bubble formation at a submerged orifice for aluminum foams produced by gas injection method [J]. Metallurgical and Materials Transaction A, 2013, 44: 729−737.
[24] LIM S C, KIM D H, KIM J S, LEE C H, YOON E P. Decomposition kinetics of machining oil and oxidation of A356.2 aluminium alloy in aluminium recycling process [J]. Materials Science and Technology, 1997, 13(10): 859−864.
[25] LONG Li-zhen, XIE Ya, HUANG Xiao-lin, LIU Xin-li, WANG Shi-liang, He Yue-hui, ZHAO Zhong-wei. Vapor-phase synthesis and mechanical properties of Al_2O_3 nanosheets [J]. Materials Science and Engineering of Powder Metallurgy, 2011, 16(6): 864−869.

吹气法泡沫铝泡壁表面氧化膜

周宇通[1]，李言祥[1,2]

1. 清华大学 材料学院，北京 100084；
2. 清华大学 先进成形制造教育部重点实验室，北京 100084

摘 要：以 A356 铝合金为原料，使用高纯氮气、空气以及氧气体积分数为 0.2%~8.0%的混合气体通过吹气法制备泡沫铝样品。利用金相显微镜、SEM 和 AES 等检测技术，研究气体中氧气含量对泡沫铝泡孔结构、相对密度、泡壁宏观及微观形貌、氧化膜覆盖面积分数和氧化膜厚度的影响。结果表明，当氧气体积分数小于 1.2%时，氧化膜覆盖面积分数随着氧气含量的上升而增加。当氧气体积分数大于 1.6%时，氧化膜覆盖了泡壁的全部表面，可以制备出泡孔结构良好的泡沫铝。由氧气体积分数为 1.6%~21%的气体制备泡沫铝泡壁的氧化膜厚度几乎不变。此外，从理论上分析氧化膜厚度不随氧气体积分数改变而改变的原因及实现氧化膜全覆盖的需氧量。最后，基于实验现象分析氧化膜在吹气法泡沫铝泡沫稳定中的作用。

关键词：泡沫铝；吹气法；氧化膜；泡沫稳定机制

(Edited by Yun-bin HE)